

## RESEARCH ARTICLE



# Analysis of Bird Strike-Induced Damage on Bio-Inspired Laminated Plates: A Comparative Study

Meryem Dilara Kop<sup>1</sup>, Aman Garg<sup>2,3</sup> and Mehmet Avcar<sup>4,\*</sup>

<sup>1</sup>Graduate School of Natural and Applied Sciences, Suleyman Demirel University, Türkiye

<sup>2</sup>Department of Civil Engineering and Smart Cities, Shantou University, China

<sup>3</sup>Department of Multidisciplinary Engineering, The NorthCap University, India

<sup>4</sup>Department of Civil Engineering, Suleyman Demirel University, Türkiye

**Abstract:** The issue of bird strikes, while seemingly straightforward, can result in significant structural and economic damage, and so it has become a hot topic. In this context, the present work aims to examine the energy absorption capacity of bio-inspired linear helicoidal (LH) laminated composite plates subjected to bird strike at various angles with the fully clamped edges. Unlike traditional impact studies, this study uses a hybrid approach that accurately captures the fluid–structure interaction during impact by combining smoothed particle hydrodynamics with finite element analysis techniques in ABAQUS software. In this framework, the energy absorption capacities of bio-inspired LH configurations are compared with those of traditional cross-ply (CPL) laminated ones having circular holes. Simulations of bird strikes are conducted using a bird density of 1000 kg/m<sup>3</sup> and a velocity of 100 m/s across various incidence angles. Hashin damage criteria are utilized to analyze fiber tension, fiber compression, and matrix tension under strike conditions. The validation results are consistent with existing literature, confirming the accuracy of the current numerical model. Strain energy analysis indicated notable variations in energy absorption characteristics across different strike angles, i.e., the bio-inspired LH laminated composite plate demonstrated greater energy absorption capacity in comparison with the traditional cross-ply laminated composite plate. LH configurations significantly outperform traditional CPL laminated composite plates, particularly at the 20-degree strike angle, where strain energy absorption is maximized. The findings provide important insights for the development of bird-strike-resistant engineering materials and structures, emphasizing the potential of bio-inspired helicoidal structures.

**Keywords:** bio-inspired laminated composites, smoothed particle hydrodynamics, finite element analysis, bird strike

## 1. Introduction

Bird strikes show a critical safety concern in aviation and aerospace engineering, with wildlife effects causing approximately \$1 billion in annual economic losses globally to the aviation industry [1–4], showing the important economic and safety implications of this phenomenon. Statistics of the Federal Aviation Administration indicate that from 1990 to 2024, wildlife strikes resulted in over 650 human fatalities and over 360 aircraft destroyed globally for both military and civil aviation [5]. Experimental characterization of bird-strike behaviors in laminated structures presents considerable challenges due to demanding requirements for time, financial, and human resources [6–11]. Addressing the existing issue through analytical methods presents significant challenges and may require considerable time investment. Consequently,

numerical approaches have become increasingly popular tools for bird-strike research [12–14]. Bird strike characteristics are soft body impacts and are different from hard body impacts, such as ballistic impacts. Soft-body impacts exhibit rare natural characteristics [15, 16]. Since bird strikes have similar impact characteristics to fluid-like impacts, the modelling of the bird strike requires a different approach, such as the smoothed particle hydrodynamics (SPH) method. SPH represents a Lagrangian approach where the material is modeled as a collection of discrete particles [17]. Recent studies of bird strikes have indicated the importance of optimization techniques designed for engineering structures. Due to the difficulties of experimental analysis of bird strike tests and high costs, computational methods combining finite element analysis (FEA) with optimization algorithms have become more critical [18].

Composite materials are extensively used in various sectors of modern technology, such as civil, automotive, and aerospace industries. Composites represent excellent corrosion resistance,

\*Corresponding author: Mehmet Avcar, Department of Civil Engineering, Suleyman Demirel University, Türkiye. Email: [mehmetavcar@sdu.edu.tr](mailto:mehmetavcar@sdu.edu.tr)

eliminating the requirement for protective coatings and reducing maintenance costs compared to metals that are susceptible to oxidation and environmental degradation [19–23]. Studies conducted in recent years have proven that the use of hybrid material combinations increases the impact resistance of composite structures. Xiang et al. [24] indicated that multilayer composite plates incorporating soft, hard, and porous materials can improve the ballistic resistance of traditional sandwich structures significantly.

Helicoidal structures, which occur naturally in living things like the mantis shrimp's puncher and some insect shells, are good at handling damage and absorbing energy [25–27]. These structures feature continuously rotating fiber orientations that provide improved toughness and crack-deflection mechanisms compared with traditional laminated composites [28–32]. Feng and Zhu [33] compared traditional sandwich panels with bio-inspired layered sandwich panels; the results showed that the newly developed bio-inspired structure exhibited better impact resistance. Zhou et al. [34] investigated three different layup laminated composites under the bird strike using the SPH-FEM analysis, and the results showed that when the plate thickness increases, the damage distribution changes from global to local, i.e., the thickest plate has the highest strain energy with lower damage energy dissipation, while the maximum damage index is not significantly affected by the thickness. Zhang et al. [35] conducted a comprehensive examination of local characteristics exhibited by bio-inspired structural systems.

In the open literature, several studies have also been conducted on the energy absorption capacities of bio-inspired laminated structures. San Ha and Lu [36] provided an extensive investigation of biologically derived structures and materials designed to improve the energy absorption capabilities of structural components. Additionally, hybridization of traditional laminates has also been investigated due to increased impact resistance. For example, Carbon Fiber Reinforced Polymer (CFRP) laminates hybridized with Kevlar and glass layers under high-velocity impact are investigated by Mousavi and Khoramshad [37], in which the results showed that positioning Kevlar layers on the back face of the laminate increased the absorbed energy by 135% with only an increase of mass by 9%. Ginzburg et al. [38] made a comparison of energy absorption capacity between helicoidal laminated composite plates and traditional laminated composite plates under low-impact velocity. Sabah et al. [39] made a comparison study of the bio-inspired laminated sandwich beams and the traditional sandwich beams using numerical and experimental analysis. Chen et al. [40] examined the high-velocity impact response of bio-inspired helicoidal composite laminates with various helix angles (15, 30, 45 degrees), and their results proved that the helicoidal mechanism is more effective under low-energy impacts compared to traditional laminates. Garg et al. [41] investigated the damage behavior of bio-inspired helicoidal laminated composite plates under two different velocities of bird impact using a hybrid SPH-FEM approach, where five different helicoidal layup configurations (exponential, recursive, semi-circular, linear, and Fibonacci) with traditional cross-ply and quasi-isotropic laminates containing circular and elliptical holes were compared. According to the published results, it can be seen that the angle of impact significantly influences the damage characteristics and energy absorption mechanisms in composite structures [42, 43]. He et al. [44] investigated the repeated impact damage behavior and damage tolerance of bio-inspired helical-structured glass fiber-reinforced polymer composites using both experimental and FEA. Baakeel et al. [45] used LS-DYNA to develop a

finite element model to study the low-velocity impact response of curved CFRP composite plates with a variety of bio-inspired configurations. Jiang et al. [46] conducted an experimental and numerical study on the low-velocity impact resistance behaviors of nonlinear rotation angle bio-inspired helicoidal composite laminates.

While many studies have been conducted on the impact resistance of composite structures, the majority of these studies concentrate on traditional laminates under simplified loading conditions. The high-speed, fluid-like behavior typical of a bird strike is not adequately represented by the current literature, which often looks at LH and traditional CPL configurations separately or focuses mostly on low-velocity impacts. Moreover, thorough comparative data using a high-fidelity hybrid SPH-FEM approach about how the energy absorption of these bio-inspired structures varies over a broad range of strike angles are noticeably lacking. The current research directly compares bio-inspired LH and traditional CPL plates with circular holes under various incidence angles in order to fill these research gaps. Furthermore, the best configurations for particular aerospace applications by assessing energy absorption capacities across different impact scenarios are clarified. To capture the intricate interaction between the fluid-like bird projectile and the laminated target, a hybrid SPH-FEA in ABAQUS/Explicit is used. Simulations of bird strikes are conducted using a bird density of  $1000 \text{ kg/m}^3$  and a velocity of 100 m/s across various incidence angles, such as 0, 10, 20, 30, 45, and 60 degrees. Hashin damage criteria are utilized to analyze fiber tension, fiber compression, and matrix tension under strike conditions.

The paper is arranged as follows: In Section 2, the materials and method are introduced. Several numerical results and discussions are given in Section 3. Main findings are summarized in Section 4.

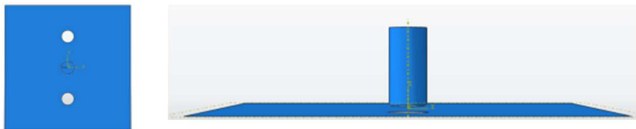
## 2. Materials and Method

According to the literature review, SPH analyses have demonstrated good agreement with soft body impact characteristics, making it suitable for bird strike simulations. Therefore, ABAQUS 2022 was employed for the SPH-FEA element analysis in this research, which have several advantages compared to the traditional finite element techniques, as follows:

- 1) The bird's material is represented by discrete particles that are free to deform and fragment. SPH successfully captures the fluid-like behavior of the bird upon impact without requiring complicated remeshing algorithms.
- 2) Because of severe element distortion, traditional Lagrangian FEM approaches are unable to adequately model the large deformations and material fragmentation that occur during high-velocity soft body impacts.
- 3) Accurate fluid-structure interaction modeling is made possible by the coupling between SPH particles (for the bird) and FEA elements (for the composite structure), and it captures the transient force distribution and energy transfer mechanisms that are essential for comprehending damage initiation and propagation in laminated composites.
- 4) The SPH-FEA methodology allows systematic parametric studies across multiple impact angles and configurations, which would be prohibitively expensive using physical testing alone, while significantly reducing costs and time requirements when compared to experimental approaches.

Here, the bio-inspired laminated composite plate is modeled using shell elements. The planar dimensions of the bio-inspired laminated composite plate are assumed to be  $1 \times 1$  m, while the thickness of 0.01 m is specified through the shell section property. The bio-inspired laminated composite plate has two circular holes located at a quarter distance from the bottom and top edges. The orientation of the plate and bird is illustrated in Figure 1.

**Figure 1**  
Bird and plate orientation



The bird is modeled as a revolved solid. The bird's dimensions are taken to be 200 mm in height and 50 mm in radius. The  $U_S - U_P$  linear Hugoniot equation state (EOS) is used in SPH model to accurately depict the projectile's fluid-like behavior upon impact. The formula for the relationship between shock velocity  $U_S$  and particle velocity  $U_P$  is  $U_S = C_0 + sU_P$ , where material constants  $c_0 = 1483$  m/s and  $s = 0$  [12]. The material properties of the laminated composite plate are taken from the study conducted by Rahimian Kolor et al. [47]. Material properties of CFRP and Hashin failure parameters are given in Tables 1, 2.

**Table 1**  
CFRP properties

Property	Value
$E_1$	105.5 GPa
$E_2 = E_3$	7.2 GPa
$G_{12} = G_{13}$	3.4 GPa
$G_{23}$	2.52 GPa
$\nu_{12} = \nu_{13}$	0.34
$\nu_{23}$	0.378
$\rho$	1500 kg/m <sup>3</sup>

**Table 2**  
Hashin failure parameters

Parameter	Value
$X_T$ (Tensile strength, longitudinal)	1340 MPa
$X_C$ (Compressive strength, longitudinal)	1192 MPa
$Y_T$ (Tensile strength, transverse)	19.6 MPa
$Y_C$ (Compressive strength, transverse)	92.3 MPa
$S_{12}$ (Shear strength, in-plane)	51 MPa
$S_{23}$ (Shear strength, out-of-plane)	23 MPa
$G_{XT}$ (Fracture energy, longitudinal tensile)	48.4 N/mm
$G_{XC}$ (Fracture energy, longitudinal compressive)	60.3 N/mm
$G_{YT}$ (Fracture energy, transverse tensile)	4.5 N/mm
$G_{YC}$ (Fracture energy, transverse compressive)	8.5 N/mm

The Hashin failure criteria implemented in the analysis are expressed as follows [19]:

Fiber tension ( $\epsilon_{11} > 0$ ):

$$R_{ft}^2 = \left( \frac{\epsilon_{11}}{X_T^\epsilon} \right)^2 + \left( \frac{\epsilon_{12}}{S_{12}^\epsilon} \right)^2 + \left( \frac{\epsilon_{13}}{S_{13}^\epsilon} \right)^2 \quad (1)$$

Fiber compression ( $\epsilon_{11} \leq 0$ ):

$$R_{fc}^2 = \left( \frac{\epsilon_{11}}{X_C^\epsilon} \right)^2 \quad (2)$$

Matrix tension ( $\epsilon_{22} + \epsilon_{33} > 0$ ):

$$R_{mt}^2 = \left( \frac{\epsilon_{11} + \epsilon_{33}}{Y_T^\epsilon} \right)^2 + \left( \frac{1}{S_{23}^\epsilon} \right)^2 \left( \epsilon_{23}^2 - \frac{E_{22}E_{33}}{(G_{23})^2} \right) (\epsilon_{22}\epsilon_{33}) + \left( \frac{\epsilon_{12}}{S_{12}^\epsilon} \right)^2 + \left( \frac{\epsilon_{13}}{S_{13}^\epsilon} \right)^2 \quad (3)$$

Matrix compression ( $\epsilon_{22} + \epsilon_{33} \leq 0$ ):

$$R_{mc}^2 = \left( \frac{E_{22}\epsilon_{11} + E_{33}\epsilon_{33}}{2G_{12}S_{12}^\epsilon} \right)^2 + \left( \frac{\epsilon_{11} + \epsilon_{33}}{Y_C^\epsilon} \right)^2 \left[ \left( \frac{E_{22}Y_C^\epsilon}{2G_{12}S_{12}^\epsilon} \right)^2 - 1 \right] + \left( \frac{1}{S_{23}^\epsilon} \right)^2 \left( \epsilon_{23}^2 - \frac{E_{22}E_{33}}{G_{23}^2} \epsilon_{22}\epsilon_{33} \right) + \left( \frac{\epsilon_{12}}{S_{12}^\epsilon} \right)^2 + \left( \frac{\epsilon_{13}}{S_{13}^\epsilon} \right)^2 \quad (4)$$

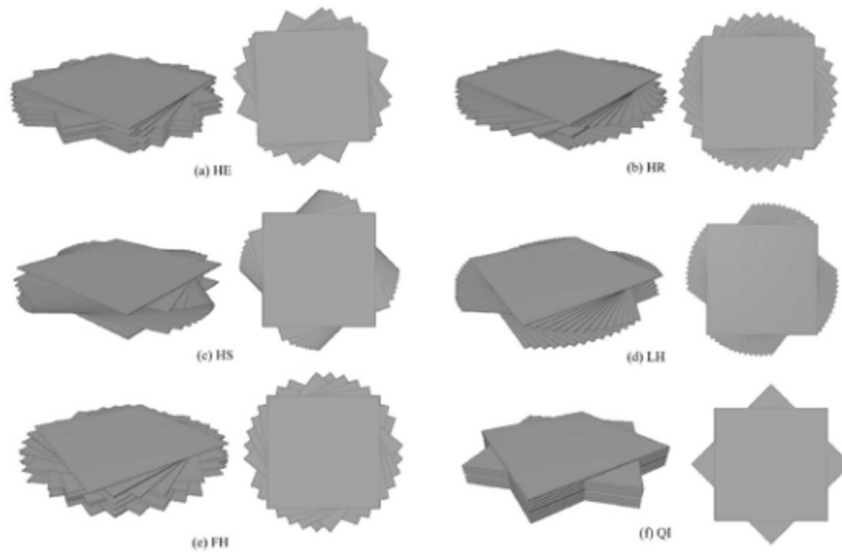
In Equation (1)-(4),  $X_T^\epsilon$  and  $X_C^\epsilon$  represent the ultimate tensile and compressive strains in the fiber direction, while  $Y_T^\epsilon$  and  $Y_C^\epsilon$  denote the corresponding values in the matrix direction. The ultimate shear strain parameters are designated as  $S_{12}^\epsilon$ ,  $S_{13}^\epsilon$ , and  $S_{23}^\epsilon$  for the respective shear modes. The ultimate tensile, compressive strains, and shear strains can be obtained as follows [41]:

$$X_T^\epsilon = \frac{X_T}{E_{11}}, X_C^\epsilon = \frac{X_C}{E_{11}}, Y_T^\epsilon = \frac{Y_T}{E_{11}}, Y_C^\epsilon = \frac{Y_C}{E_{11}}, S_{12}^\epsilon = \frac{S_{12}}{G_{12}}, S_{13}^\epsilon = \frac{S_{13}}{G_{13}}, S_{23}^\epsilon = \frac{S_{23}}{G_{23}} \quad (5)$$

In the present research, the laminated composite plate is assumed to have clamped boundary conditions applied along all four edges, thereby restricting both translational and rotational degrees of freedom. The finite element simulations are carried out using the dynamic explicit analysis procedure available in Abaqus/Explicit. The total duration of the analysis is set to 0.01 s. Numerical simulations are conducted using the dynamic explicit analysis procedure. The laminated composite plates analyzed in this study are assumed to consist of a 64-ply laminated structure with two configurations: LH laminated composite and traditional CPL. The scheme of LH laminated composite is illustrated in Figure 2. The orientation scheme of the laminated composite plate is taken from the study of Garg et al. [48].

The bird model is characterized by a density of 1000 kg/m<sup>3</sup> and a velocity of 100 m/s. Numerical analyses are performed, including 0, 10, 20, 30, 45, and 60 degrees. The stacking sequence of the present bio-inspired laminated composite plates is defined mathematically according to the study of Garg et al. [41]: LH:  $\theta_1/\theta_2/\theta_3/\dots/\theta_n = (n-1)\xi$ .  $\xi$  is taken as 4 for the configuration. For the bio-inspired laminated composite plate, a quad-dominated mesh with an element size of 0.01 is used.

**Figure 2**  
Scheme of bio-inspired laminated composites



### 3. Numerical Results and Discussion

**Example 1:** In Figure 3, the findings for the strain energy and time graph of the LH configuration are compared with those of Garg et al. [41]. As one can see from the results, the peak points and graph behaviors of both results are similar, which validates the accuracy of the present results.

**Example 2:** In Figure 4, the findings for the strain energy and time graph of the traditional CPL laminated composite are compared with those of Garg et al. [41]. As one can see from the results, the strain energy characteristics of the reference study and the present study are similar, which proves the accuracy of the present results.

**Example 3:** After the bird strike, damages occurred in fiber tension, matrix tension, and Hashin fiber and matrix. Figure 5 shows the comparison of initiation criteria with the results of Garg et al. [41] for the bio-inspired linear helicoidal laminated composite plate. The current study's results are highly consistent with earlier study on bio-inspired laminated composites. In particular, the LH configurations' superiority over traditional CPL laminates is consistent with the findings published by

**Figure 3**  
The comparison of the strain energy–time graph for bio-inspired LH laminated composite plates

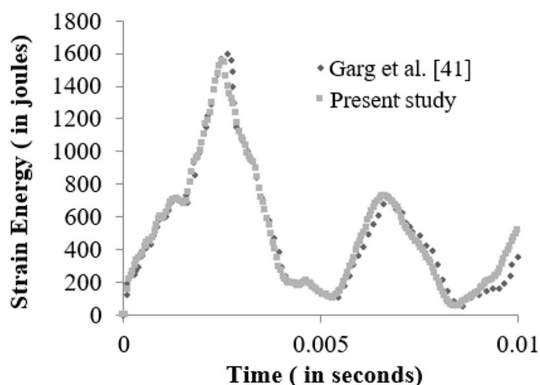
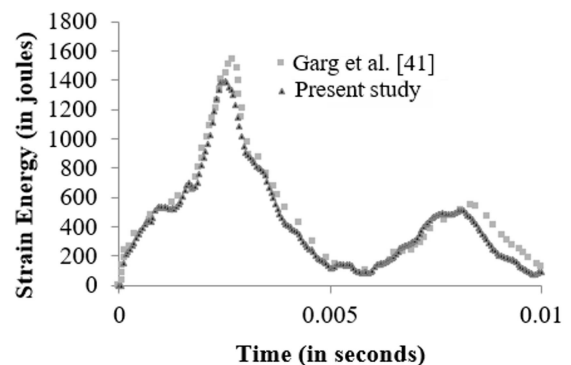


**Figure 4**  
The comparison of the strain energy–time graph for CPL laminated composite plates



Garg et al. [41], who highlighted the helicoidal structures' increased resistance to damage.

In Figures 3-5, the validation step is carried out successfully for both LH and conventional CPL configurations, and the accuracy of the present model is proven. Although the authors concentrated on the overall impact response, the present research expands on these conclusions by showing that this benefit endures over a broad range of incidence angles, with peak efficiency taking place at 20°. The bio-inspired design's capacity to reduce localized impact damage is further supported by the fact that the crack deflection mechanisms and energy dissipation patterns seen in the current LH models agree with the physical explanations offered by Xiang et al. [24]. The hybrid SPH-FEA approach successfully captures the intricate interaction between the fluid-like bird projectile and the helicoidal target, as demonstrated quantitatively by the small deviation from established literature (approximately 2% for LH and 7% for CPL).

After the validation steps, how the energy absorption capacity changed depending on the bird strike angle is investigated. Related to the angle of the bird's strike, energy absorption capacity exhibits different variations.

**Figure 5**  
The comparison of damages occurred in the bio-inspired LH laminated composite plate

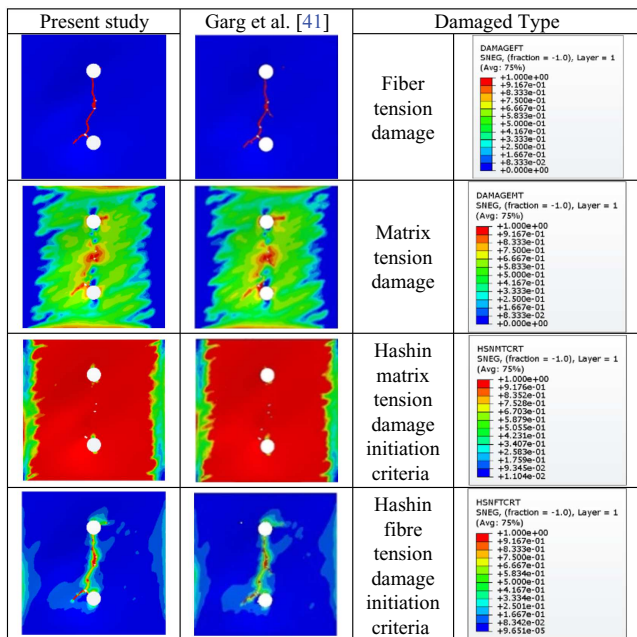
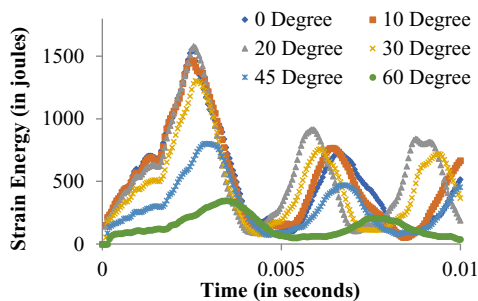


**Figure 6**  
Strain energy–time graph for different strike angles on bio-inspired LH laminated composite plate

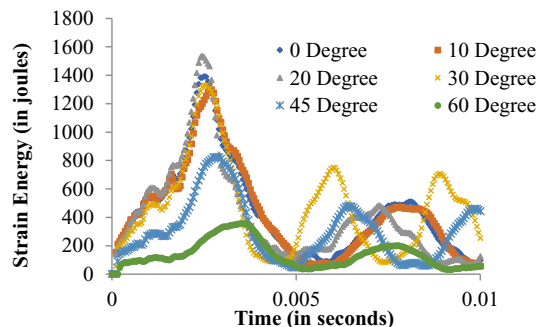


**Example 4:** As shown in Figure 6 for the LH configuration, the 20-degree angle has the maximum strain energy value, which is 1580.61 J. For the other five strike angles (0, 10, 30, 45, and 60 degrees), peak strain energy values are 1551.40 J, 1466.60 J, 1303.09 J, 801.35 J, and 347.21 J. However, at 0.01 seconds, energy values are 188.9377 J, 517.2037 J, 667.1972 J, 368.2618 J, 455.9052 J, and 37.71353 J. Energy dissipation values are 88.0%, 66.7%, 54.5%, 71.7%, 43.1%, and 89.1%.

**Example 5:** Similarly, with the LH configuration traditional CPL configuration, when a bird strike occurs at 20 degrees, it produces maximum strain energy of 1534.542 J, as shown in Figure 7. Peak values are 1390.776 J, 1299.584 J, 1329.181 J, 823.1891 J, and 356.2488 J for 0, 10, 30, 45, and 60 degrees, respectively, with corresponding final values of 125.2604 J, 95.20317 J, 57.97625 J, 253.0825 J, 441.8676 J, and 55.42315 J, energy dissipation percentages are 91.8%, 93.2%, 95.5%, 81.0%, 46.3%, and 84.4% at 0.01 s.

Numerical results demonstrated that the bio-inspired plates with LH laminated configurations show the best energy absorption performance at 20 degrees by 3% and at 0 degrees by 12%,

**Figure 7**  
Strain energy–time graph for different strike angles on a traditional CPL laminated composite plate



whereas CPL configurations showed better energy dissipation performance at low bird strike angles. For both configurations, the time to reach peak strain energy values increases with steeper bird strike angles.

#### 4. Conclusion

The present study investigated the energy absorption capacity of the bio-inspired linear helicoidal laminated composite plate, and comparisons are performed with the traditional CPL composite configurations with six strike angles using SPH-FEA under fully clamped boundary conditions. The validation research has been concluded using findings from finite element studies in the literature for both traditional cross-ply laminated composite plates and LH laminated composite plates.

In summary, the subsequent conclusions are provided:

- 1) Both configurations showed the highest energy absorption performance at the 20-degree bird strike.
- 2) LH configurations exhibit better peak energy absorption at the 0-degree bird strike.
- 3) CPL has better energy dissipation capability at lower angles rather than the higher ones.

Consequently, in aerospace sectors, the use of linear helicoidal laminated composites can be preferable for aircraft leading edges owing to their enhanced resistance to perpendicular impacts; for example, CPL design can be utilized for engine intake components that need optimal energy dissipation characteristics.

This research is limited to a velocity parameter and a hole diameter, a boundary condition, a layup configuration, and an aspect ratio for the bio-inspired laminated composite plate. Therefore, the current research will be extended by considering several new parameters for the considered structure, such as varying velocity, hole and aspect ratio parameters, different boundary conditions, and layup configurations.

#### Ethical Statement

This study does not contain any studies with human or animal subjects performed by any of the authors.

#### Conflicts of Interest

Mehmet Avcar is the Editorial Board Member for Archives of Advanced Engineering Science, and was not involved in the

editorial review or the decision to publish this article. The authors declare that they have no conflicts of interest to this work.

## Data Availability Statement

Data sharing is not applicable to this article, as no new data were created or analyzed in this study.

## Author Contribution Statement

**Meryem Dilara Kop:** Conceptualization, Methodology, Software, Validation, Formal analysis, Investigation, Resources, Data curation, Writing – original draft, Visualization. **Aman Garg:** Conceptualization, Methodology, Software, Investigation, Data curation, Supervision, Project administration. **Mehmet Avcar:** Conceptualization, Methodology, Investigation, Resources, Data curation, Writing – original draft, Writing – review & editing, Supervision, Project administration.

## References

- [1] Boyacı, E., & Altın, M. (2023). Experimental and numerical approach on bird strike: A review. *International Journal of Automotive Science and Technology*, 7(2), 95–103. <https://doi.org/10.30939/ijastech..1293572>
- [2] Konik, R., Kassapoglou, C., & Nguyen, D. (2023). Design analysis and testing of flat sandwich panels under bird strike. *Journal of Sandwich Structures & Materials*, 25(1), 144–163. <https://doi.org/10.1177/10996362221127968>
- [3] Chen, S. Y., Van de Waerdt, W., & Castro, S. G. (2023). Design for bird strike crashworthiness using a building block approach applied to the Flying-V aircraft. *Heliyon*, 9(4), e14723. <https://doi.org/10.1016/j.heliyon.2023.e14723>
- [4] Doubrava, R., Vlach, J., Oberthor, M., Vich, O., & Bělský, P. (2024). Bird strike tests, analyses, and design optimisation of a tilt-rotor aircraft composite inlet. *Engineering Failure Analysis*, 161, 108244. <https://doi.org/10.1016/j.engfailanal.2024.108244>
- [5] Dolbeer, R. A., Begier, M. J., Miller, P. R., Weller, J. R., & Anderson, A. L. (2025). *Wildlife strikes to civil aircraft in the United States, 1990-2024: 31th Annual Report. Federal Aviation Administration, Office of Airport Safety and Standards, Airport Safety & Certification Program.* [https://www.faa.gov/airports/airport\\_safety/wildlife/wildlife-strike-report-1990-2024](https://www.faa.gov/airports/airport_safety/wildlife/wildlife-strike-report-1990-2024)
- [6] Le, V. T., Jin, T., & Goo, N. S. (2022). Mechanical behaviors and fracture mechanisms of CFRP sandwich composite structures with bio-inspired thin-walled corrugated cores. *Aerospace Science and Technology*, 126, 107599. <https://doi.org/10.1016/j.ast.2022.107599>
- [7] Shi, Y., Jia, J., Lin, R., Chen, J., Fang, X., & Sheng, Y. (2026). Research on spatiotemporal risk assessment model of bird strike at airports and precise prevention and control strategies. *Scientific Reports*, 16, 6449. <https://doi.org/10.1038/s41598-026-36814-6>
- [8] Liu, Z., Xu, Y., Huang, F., Wu, Z., Li, Y., & Liu, J. (2026). Test and numerical simulation on fragmentation behavior of an aircraft PMMA windshield under bird strike by using a novel coupled SPH-DEM method. *Aerospace Science and Technology*, 173, 111742. <https://doi.org/10.1016/j.ast.2026.111742>
- [9] Liu, S., Zhang, X., Feng, Y., Zhao, X., Liu, J., & Li, G. (2026). A novel bird strike model incorporating soft and skeletal tissues for impact damage of aircraft engine blades. *Computational Particle Mechanics*, 13, 154–171. <https://doi.org/10.1016/j.cpm.2026.01.004>
- [10] Zhang, C., Cao, M., Ma, W., Huang, F., Liu, Z., Li, Y., & Liu, J. (2026). Numerical simulation and validation on hydrodynamic models for artificial bird impacted with aircraft structures. *Chinese Journal of Aeronautics*, 104163. <https://doi.org/10.1016/j.cja.2026.104163>
- [11] Zhang, H., Hu, R., Zhao, Q., Cao, W., & Zhang, C. (2025). Effect of bird strike on residual strength and vibration of fan blades for aero-engines. *Aerospace Science and Technology*, 168, 110925. <https://doi.org/10.1016/j.ast.2025.110925>
- [12] Yang, Q., Jones, V., & McCue, L. (2012). Free-surface flow interactions with deformable structures using an SPH-FEM model. *Ocean engineering*, 55, 136–147. <https://doi.org/10.1016/j.oceaneng.2012.06.031>
- [13] Li, J., Lou, Y., Chai, X., Ma, Z., & Jin, X. (2022). Numerical simulation of bird strike on jet engine considering bird ingestion requirements. *Journal of Aircraft*, 59(3), 761–773. <https://doi.org/10.2514/1.C036076>
- [14] Zhang, C., Lu, G., & Suo, T. (2023). Impact dynamics for advanced aerospace materials and structures. *Journal of Aerospace Engineering*, 36(4). <https://doi.org/10.1061/JAEEZ.ASENG-5047>
- [15] Barber, J. P., Taylor, H. R., & Wilbeck, J. S. (1975). *Characterization of bird impacts on a rigid plate: Part 1.* AFFDLTR755
- [16] Wilbeck, J. S. (1977). *Impact behavior of low strength projectiles.* USA: Texas A&M University.
- [17] Huang, X. T., Sun, P. N., Lyu, H. G., & Zhong, S. Y. (2023). Study of 3D self-propulsive fish swimming using the  $\delta^+$ -SPH model. *Acta Mechanica Sinica*, 39(1), 722053. <https://doi.org/10.1007/s10409-022-22053-x>
- [18] Timhede, V., Timhede, S., Winyangkul, S., & Slesongsom, S. (2025). Aircraft wing design against bird strike using metaheuristics. *Aerospace*, 12(5), 436. <https://doi.org/10.3390/aerospace12050436>
- [19] Campbell, F. C. (2010). *Structural composite materials.* ASM International.
- [20] Skoczylas, J., Kłonica, M., & Samborski, S. (2026). Recent advances in application of composite materials in the aerospace industry. *Advances in Science and Technology. Research Journal*, 20(4), 475–491. <https://doi.org/10.12913/22998624/214594>
- [21] Birhan, M., Negash, B., Batu, T., & Abunu, Y. (2026). Integrating composite materials throughout the military sector: A review. *Advances in Materials Science and Engineering*, 2026(1), 9931653. <https://doi.org/10.1155/amse/9931653>
- [22] İkinci, B. (2025). Manufacturing methods of functionally graded materials: A comprehensive review. *Journal of Ceramics and Composites*, 1(1), 6–20.
- [23] Sayyad, A., & Wagh, H. (2025). A review of production techniques, classifications, material gradation rules, and industrial applications of functionally graded materials. *Journal of Ceramics and Composites*, 2(1), 23–57.
- [24] Xiang, C., Yang, B., Yu, X., Yang, Y., & Li, X. (2025). Ballistic resistance of multilayer composite plates comprising soft, hard, and porous materials. *Structures*, 80, 109613. <https://doi.org/10.1016/j.istruc.2025.109613>
- [25] Xu, Y., & Feng, D. (2025). Enhancing impact resistance of fiber-reinforced polymer composites through bio-inspired helicoidal structures: A review. *Polymer Composites*, 46(7), 5823–5856. <https://doi.org/10.1002/pc.29352>

- [26] Sharma, A., Tonk, A., Garg, A., Li, L., & Chalak, H. D. (2023). First-ply failure analysis of bioinspired double and cross-helicoidal laminated sandwich plates. *American Institute of Aeronautics and Astronautics Journal*, 61(11), 5087–5095. <https://doi.org/10.2514/1.J063176>
- [27] Siddiqui, M. S., Rabbi, M. S., Ahmed, R. U., Alam, F., Hossain, M. A. M., Ahsan, S., & Miah, N. M. (2025). Bioinspired composite structures: A comprehensive review of natural materials, fabrication methods, and engineering applications. *Composites Part C: Open Access*, 17, 100578. <https://doi.org/10.1016/j.jcomc.2025.100578>
- [28] Wijerathne, B., Liao, T., Ostrikov, K., & Sun, Z. (2022). Bioinspired robust mechanical properties for advanced materials. *Small Structures*, 3(9), 2100228. <https://doi.org/10.1002/sstr.202100228>
- [29] Berhie, S. E., Chunt, C., Kassa, M. K., & Bodduru, K. (2026). Mechanical behavior of bio-inspired laminated MXene Reinforced GFRP composite core of structural sandwich panels: Numerical and experimental study. *Polymer Composites*, 47(1), 212–230. <https://doi.org/10.1002/pc.70139>
- [30] Snell-Rood, E. C., & Smirnoff, D. (2023). Biology for biomimetics I: Function as an interdisciplinary bridge in bio-inspired design. *Bioinspiration & Biomimetics*, 18(5), 052001.
- [31] Geronel, R. S., & Bueno, D. D. (2025). An overview on bio-inspired UAVs: State-of-the art, challenges and opportunities. *Proceedings of the Institution of Mechanical Engineers, Part G: Journal of Aerospace Engineering*, 239(12), 1293–1308. <https://doi.org/10.1177/09544100251329987>
- [32] Rajput, V., Mulay, P., & Mahajan, C. M. (2025). Bio-inspired algorithms for feature engineering: Analysis, applications and future research directions. *Information Discovery and Delivery*, 53(1), 56–71. <https://doi.org/10.1108/IDD-11-2022-0118>
- [33] Feng, X., & Zhu, P. (2024). Study of impact resistance of a novel bio-inspired ceramic-composite structure using finite element simulations. *Mechanics of Advanced Materials and Structures*, 31(25), 7420–7433. <https://doi.org/10.1080/15376494.2023.2245813>
- [34] Zhou, Y., Sun, Y., Huang, T., & Cai, W. (2019). SPH-FEM simulation of impacted composite laminates with different layups. *Aerospace science and technology*, 95, 105469. <https://doi.org/10.1016/j.ast.2019.105469>
- [35] Zhang, B., Han, Q., Zhang, J., Han, Z., Niu, S., & Ren, L. (2020). Advanced bio-inspired structural materials: Local properties determine overall performance. *Materials today*, 41, 177–199. <https://doi.org/10.1016/j.matmod.2020.04.009>
- [36] San Ha, N., & Lu, G. (2020). A review of recent research on bio-inspired structures and materials for energy absorption applications. *Composites Part B: Engineering*, 181, 107496. <https://doi.org/10.1016/j.compositesb.2019.107496>
- [37] Mousavi, M. V., & Khoramishad, H. (2020). Investigation of energy absorption in hybridized fiber-reinforced polymer composites under high-velocity impact loading. *International Journal of Impact Engineering*, 146, 103692. <https://doi.org/10.1016/j.ijimpeng.2020.103692>
- [38] Ginzburg, D., Pinto, F., Iervolino, O., & Meo, M. (2017). Damage tolerance of bio-inspired helicoidal composites under low velocity impact. *Composite Structures*, 161, 187–203. <https://doi.org/10.1016/j.compstruct.2016.10.097>
- [39] Sabah, S. A., Kueh, A. B. H., & Al-Fasih, M. Y. (2017). Comparative low-velocity impact behavior of bio-inspired and conventional sandwich composite beams. *Composites Science and Technology*, 149, 64–74. <https://doi.org/10.1016/j.compscitech.2017.06.014>
- [40] Chen, W., Lin, H., Li, M., Zhang, Y., Huang, H., Wu, X., & Li, X. (2025). High-velocity impact response and damage behavior of bio-inspired helicoidal composite laminates: Experimental and numerical investigation. *Polymer Composites*, 46(10), 9148–9160. <https://doi.org/10.1002/pc.29546>
- [41] Garg, A., Shukla, N. K., Belarbi, M. O., Mukherjee, D., Pushpavalli, M., Raman, R., . . . , & Li, L. (2025). Bird strike-induced damage studies on bio-inspired laminated plates with holes. *Aerospace Science and Technology*, 162, 110200. <https://doi.org/10.1016/j.ast.2025.110200>
- [42] Guida, M., Marulo, F., Meo, M., Grimaldi, A., & Olivares, G. (2011). SPH–Lagrangian study of bird impact on leading edge wing. *Composite Structures*, 93(3), 1060–1071. <https://doi.org/10.1016/j.compstruct.2010.10.001>
- [43] Zhang, D., & Fei, Q. (2016). Effect of bird geometry and impact orientation in bird striking on a rotary jet-engine fan analysis using SPH method. *Aerospace Science and Technology*, 54, 320–329. <https://doi.org/10.1016/j.ast.2016.05.003>
- [44] He, L., Yao, Z., Jiang, L., Guo, Z., & Lyu, Q. (2025). Repeated impact damage behavior and damage tolerance of bio-inspired helical-structured glass fiber resin matrix composites. *Polymers*, 17(13), 1720. <https://doi.org/10.3390/polym17131720>
- [45] Baakeel, F. K., Eltaher, M. A., & Basha, M. A. (2024). Impact response of bio-inspired curved laminated composite plates: A numerical simulation. *Advances in Aircraft and Spacecraft Science*, 11(4), 331–361.
- [46] Jiang, H., Ren, Y., Liu, Z., Zhang, S., & Lin, Z. (2019). Low-velocity impact resistance behaviors of bio-inspired helicoidal composite laminates with non-linear rotation angle based layups. *Composite Structures*, 214, 463–475. <https://doi.org/10.1016/j.compstruct.2019.02.034>
- [47] Rahimian Kolor, S. S., Karimzadeh, A., Yidris, N., Petrù, M., Ayatollahi, M. R., & Tamin, M. N. (2020). An energy-based concept for yielding of multidirectional FRP composite structures using a mesoscale lamina damage model. *Polymers*, 12(1), 157. <https://doi.org/10.3390/polym12010157>
- [48] Garg, A., Fantuzzi, N., Avcar, M., & Li, L. (2025). High-fidelity surrogate-driven h-refined IGA for free vibration analysis of laminated composite annular plates with radial and curved cracks. *Archives of Civil and Mechanical Engineering*, 25(4), 225. <https://doi.org/10.1007/s43452-025-01269-5>

**How to Cite:** Kop, M. D., Garg, A., & Avcar, M. (2026). Analysis of Bird Strike-Induced Damage on Bio-Inspired Laminated Plates: A Comparative Study. *Archives of Advanced Engineering Science*. <https://doi.org/10.47852/bonviewAAES62028112>